

Minimal Vectorlike Model In Supersymmetric Unification

Sibo Zheng*

Department of Physics, Chongqing University, Chongqing 401331, China

(Dated: April 26, 2019)

In comparison with the minimal supersymmetry, an extension by vectorlike fermions is able to explain the Higgs mass while retaining the grand unification. In this paper, we study the minimal vectorlike model by focusing on the vectorlike leptons. We derive the mass spectrum in the electroweak sector, calculate the effects on the Higgs physics such as one-loop radioactive correction to Higgs mass and Higgs self coupling, and address the signals of either vectorlike or neutralino dark matter. Collider constraints on the vectorlike leptons at the LHC are also briefly discussed.

I. INTRODUCTION

With the 125 GeV Higgs scalar [1, 2] established at the Large Hadron Collider (LHC), identifying the nature of this Higgs which will reveal the origin of electroweak symmetry breaking (EWSB), is one of prior tasks at this facility. In the literature, there are various classes of scenarios to naturally explain the EWSB, among which supersymmetry (SUSY) have attracted marvelous attention after the discovery of Higgs. Unfortunately, the prospective on the minimal supersymmetry standard model (MSSM) is rather pessimistic. The main reasons for this include that some of mass parameters related to the third generation of SM fermions have to be at least of order several TeVs [3, 4], and signals of neutralino are yet observed at any facilities of dark matter direct detection [5, 6].

In order to reduce the stress on MSSM, various extensions are advocated, of which vectorlike (VL) fermions are of special interest because of the following features.

- First of all, VL fermions are one of viable extensions which retain the perturbative unification [7, 8] similar to the next-to-minimal supersymmetric model (NMSSM).
- Secondly, the naturalness issue imposed by 125 GeV Higgs mass in the MSSM can be solved by new radioactive correction due to VL fermions with mass of order TeV scale [9–11], which differs from the NMSSM in which the Higgs mass is corrected at the tree level.
- Finally, the strong constraint on neutralino dark matter from dark matter direct detection can be relaxed due to new neutral fermions in the VL sector.

In this paper, we will consider the minimal VL model as described in Table.I. We explore this model by focusing on the VL leptons therein, which is composed of one singlet and two doublets. In this model, the VL leptons directly couple to the Higgs doublets rather than the SM leptons, which implies that they have important roles to

VL model	Representation
Minimal	$\mathbf{1} + \mathbf{5} + \bar{\mathbf{5}}$
LND [9]	$\mathbf{1} + \mathbf{1} + \mathbf{5} + \bar{\mathbf{5}}$
VL 4th – gen [11]	$\mathbf{1} + \mathbf{5} + \bar{\mathbf{5}} + \mathbf{10} + \bar{\mathbf{10}}$

TABLE I: TeV-scale VL models and their representations under $SU(5)$.

play in phenomenologies of both Higgs physics and dark matter.

The paper is organized as follows. In Sec.II we introduce the minimal VL model, derive the EWSB conditions, and calculate mass spectrum in the electroweak sector for later purposes. Sec.III is devoted to estimate effects on Higgs physics, where the one-loop radioactive correction to Higgs mass and the modification on Higgs self coupling is presented in Sec.IIIA and Sec.IIIB, respectively. In Sec.IV, we will discuss dark matter physics in the presence of VL leptons. In particular, in Sec.IVA we will show the VL dark matter is excluded by large Yukawa coupling as required by the Higgs mass; whereas the parameter space of neutralino dark matter is expanded mainly due to the relaxed Higgs mass constraint. In Sec.V, the collider constraint on the VL leptons will be briefly addressed. Finally, we conclude in Sec.VI.

II. THE MODEL

In the minimal VL model, the matter content contains a singlet N , two down-type quarks D and \bar{D} , and two VL doublets L and \bar{L} with hyper charge $1/2$ and $-1/2$, respectively. These matters constitute a $\mathbf{5}$ and $\bar{\mathbf{5}}$ representation of $SU(5)$ consistent with $SU(5)$ unification [7, 8].

The superpotential for the VL lepton sector reads as,

$$W_{VL} = k H_u \bar{L} N - h L H_d N + M_L \bar{L} L + \frac{1}{2} M_N N^2 \quad (1)$$

where $M_{L,N}$ refer to VL masses and k and h are Yukawa coupling constants. The superpotential for MSSM is given by,

$$W_{\text{MSSM}} = Y_u q \bar{u} H_u + Y_d q \bar{d} H_d + Y_e l \bar{e} H_d + \mu H_u H_d. \quad (2)$$

*Electronic address: sibozheng.zju@gmail.com

Although the matter content of the minimal VL model is similar to that of NMSSM with two additional doublets [12], they are still different, as seen from the superpotentials Eq.(1) and Eq.(2), which have an interpretation of unification.

Apart from the extension on the superpotential, the soft mass Lagrangian $\mathcal{L}_{\text{soft}}$ is also expanded as,

$$-\mathcal{L}_{\text{soft}} \supset -\mathcal{L}_{\text{soft}}^{\text{MSSM}} + m_L |L|^2 + m_{\bar{L}} |\bar{L}|^2 + m_N |N|^2 + (kA_k H_u \bar{L} N - hA_h L H_d N + \text{H.c.}), \quad (3)$$

where $m_{L,N,D}$ and $A_{k,h}$ represent soft mass parameters, and $\mathcal{L}_{\text{soft}}^{\text{MSSM}}$ contains MSSM soft masses such as

$$-\mathcal{L}_{\text{soft}}^{\text{MSSM}} = m_{H_u}^2 |H_u|^2 + m_{H_d}^2 |H_d|^2 + (bH_u H_d + \text{H.c.}).$$

Following the notation and conventions in [13], we express the Higgs and VL doublets as, respectively,

$$\begin{aligned} H_u &= \begin{pmatrix} H_u^+ \\ H_u^0 \end{pmatrix} = \begin{pmatrix} H_u^+ \\ v_u + \frac{1}{\sqrt{2}}(H_{uR}^0 + iH_{uI}^0) \end{pmatrix} \\ H_d &= \begin{pmatrix} H_d^0 \\ H_d^- \end{pmatrix} = \begin{pmatrix} v_d + \frac{1}{\sqrt{2}}(H_{dR}^0 + iH_{dI}^0) \\ H_d^- \end{pmatrix} \end{aligned} \quad (4)$$

and

$$\begin{aligned} L &= \begin{pmatrix} E^+ \\ \eta \end{pmatrix} = \begin{pmatrix} E^+ \\ v_L + \frac{1}{\sqrt{2}}(\eta_R + i\eta_I) \end{pmatrix} \\ \bar{L} &= \begin{pmatrix} \bar{\eta} \\ E^- \end{pmatrix} = \begin{pmatrix} \bar{v}_L + \frac{1}{\sqrt{2}}(\bar{\eta}_R + i\bar{\eta}_I) \\ E^- \end{pmatrix} \end{aligned} \quad (5)$$

Similarly, we write singlet N as

$$N = n + \frac{1}{\sqrt{2}}(N_R + iN_I). \quad (6)$$

Mass parameters $v_{u,d}$, v_L , \bar{v}_L and n denote the vacuum expectation values (vevs).

These vevs are determined by the minimization of scalar potential V as given by

$$V = V_F + V_D - \mathcal{L}_{\text{soft}} \quad (7)$$

where

$$\begin{aligned} V_F &= |\mu H_d + k\bar{L}N|^2 + |\mu H_u - hLN|^2 \\ &\quad + |M_L \bar{L} - hH_d N|^2 + |kH_u N + M_L L|^2 \\ &\quad + |kH_u \bar{L} - hLH_d + M_N N|^2, \\ V_D &= \frac{g_1^2 + g_2^2}{8} (|H_u|^2 - |H_d|^2 + |L|^2 - |\bar{L}|^2)^2 \\ &\quad + \frac{g_2^2}{2} |H_u H_d^\dagger + L \bar{L}^\dagger|^2 \end{aligned} \quad (8)$$

Here, g_1 and g_2 refers to $U(1)_Y$ and $SU(2)_L$ gauge coupling constant, respectively. After substituting Eq.(5) and Eq.(6) into Eq.(7), we have the EWSB conditions:

$$\begin{aligned} 0 &= F_N(-k\bar{v}_L) + F_{\bar{L}}(kn) + F_{H_d}\mu - kA_k n\bar{v}_L + m_{H_u}^2 v_u - \frac{1}{2}M_Z^2 \cos 2\beta v_u(1-\delta) - b \cot \beta v_u \\ 0 &= F_N(hv_L) + F_L(-hn) + F_{H_u}\mu + hA_h n v_L + m_{H_d}^2 v_d + \frac{1}{2}M_Z^2 \cos 2\beta v_d(1-\delta) - b \tan \beta v_d \\ 0 &= h^2 n^2 v_L + F_N(hv_d) + hA_h n v_d + m_L^2 v_L - \frac{1}{2}M_Z^2 \cos 2\gamma v_L \delta \\ 0 &= k^2 n^2 \bar{v}_L + F_N(-kv_u) - kA_k n v_u + m_{\bar{L}}^2 \bar{v}_L + \frac{1}{2}M_Z^2 \cos 2\gamma \bar{v}_L \delta \\ 0 &= F_N M_N + F_L(-hv_d) + F_{\bar{L}}(kv_u) + n(k^2 \bar{v}_L^2 + h^2 v_L^2) - kA_k v_u \bar{v}_L + hA_h v_d v_L + m_N^2 n, \end{aligned} \quad (9)$$

where small cross terms from D -terms have been ignored for simplicity. In Eq.(9) $\tan \beta$, $\tan \gamma$ and δ are defined as

$$\begin{aligned} \tan \gamma &= \frac{v_L}{\bar{v}_L}, & \delta &= \frac{v_L^2 + \bar{v}_L^2}{(v/\sqrt{2})^2}, \\ \tan \beta &= \frac{v_u}{v_d}, & 1 - \delta &= \frac{v_u^2 + v_d^2}{(v/\sqrt{2})^2}. \end{aligned} \quad (10)$$

The SM expectation value for weak scale $v \simeq 246$ GeV.

With the conditions of EWSB described in Eq.(9), we can directly derive the scalar and fermion mass spec-

trum in the electroweak sector. We refer the reader to appendix A and B for scalar mass spectrum such as CP-even, CP-odd, and CP-charged scalars, and fermion mass spectrum such as neutralinos and charginos, respectively. In the next section, we will discuss constraints on the model parameters from precision measurements on the Higgs couplings.

	Parameter	Fit
k_t	$\frac{1}{\sqrt{1-\delta}} \frac{ \mathcal{O}_{11} }{s_\beta}$	$0.81^{+0.19}_{-0.15}$
k_b	$\frac{1}{\sqrt{1-\delta}} \frac{ \mathcal{O}_{12} }{c_\beta}$	$0.74^{+0.33}_{-0.29}$
k_τ	$\frac{1}{\sqrt{1-\delta}} \frac{ \mathcal{O}_{21} }{c_\beta}$	$0.84^{+0.19}_{-0.18}$
k_W	$\sqrt{1-\delta}(s_\beta \mathcal{O}_{11} + c_\beta \mathcal{O}_{12}) + \sqrt{\delta}(s_\gamma \mathcal{O}_{13} + c_\gamma \mathcal{O}_{14})$	$0.95^{+0.14}_{-0.13}$
k_Z	$\sqrt{1-\delta}(s_\beta \mathcal{O}_{11} + c_\beta \mathcal{O}_{12}) + \sqrt{\delta}(s_\gamma \mathcal{O}_{13} + c_\gamma \mathcal{O}_{14})$	$1.05^{+0.16}_{-0.16}$
vev	$v\sqrt{1-\delta}$	245 ± 15

TABLE II: LHC constraints from global fits to SM-like Higgs couplings [20] and weak scale v [17] at 68% CL in unit of GeV.

III. HIGGS PHYSICS

A. Higgs Couplings

The precision measurement on the Higgs couplings is one of major tasks at the LHC, for it reveals the pattern of EWSB in the sense that different new physics models predict different sets of Higgs couplings. In particular, LHC has verified the SM-like Higgs coupling to SM fermions such as b [14] and τ [15] as well as couplings to SM vector bosons such as W [16]. Alternatively, these measurements tell us to what extension [17] v is deviated from its SM expectation value. Such data will be further improved in higher level of precision at the future HL-LHC [18] or ILC [19] in preparation.

The Higgs couplings to SM particles in our model are given as,

$$\begin{aligned}
y_t &= \frac{m_t}{v} \frac{\mathcal{O}_{11}}{\sqrt{1-\delta}s_\beta}, \\
y_b &= \frac{m_b}{v} \frac{\mathcal{O}_{12}}{\sqrt{1-\delta}c_\beta}, \\
y_\tau &= \frac{m_\tau}{v} \frac{\mathcal{O}_{12}}{\sqrt{1-\delta}c_\beta}, \\
y_W &= \frac{2M_W^2}{v} \left[\sqrt{1-\delta}(s_\beta \mathcal{O}_{11} + c_\beta \mathcal{O}_{12}) + \sqrt{\delta}(s_\gamma \mathcal{O}_{13} + c_\gamma \mathcal{O}_{14}) \right], \\
y_Z &= \frac{M_Z^2}{v} \left[\sqrt{1-\delta}(s_\beta \mathcal{O}_{11} + c_\beta \mathcal{O}_{12}) + \sqrt{\delta}(s_\gamma \mathcal{O}_{13} + c_\gamma \mathcal{O}_{14}) \right],
\end{aligned} \tag{11}$$

where the constant coefficients are the SM values. An orthogonal matrix \mathcal{O} is introduced to diagonalize the CP-even mass matrix \mathcal{M}_S^2 in appendix A, with components \mathcal{O}_{1j} in the SM-like Higgs scalar h_1 defined as

$$h_1 = \mathcal{O}_{11}H_{uR}^0 + \mathcal{O}_{12}H_{dR}^0 + \mathcal{O}_{13}\eta_R + \mathcal{O}_{14}\bar{\eta}_R + \mathcal{O}_{15}N_R. \tag{12}$$

According to global fits to the LHC measurements on Higgs couplings, we obtain the constraints on model parameters in Eq.(11), which are summarized in Table.II. The constraint on the weak scale suggests a small parameter range for δ ,

$$0 \leq \delta \leq 0.12, \tag{13}$$

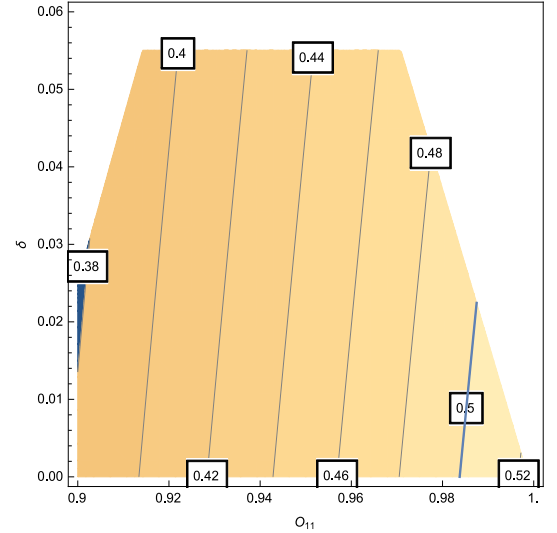


FIG. 1: The contour of $\lambda_{3h}/\lambda_{3h}^{\text{SM}}$ as function of δ and \mathcal{O}_{11} for $\tan\beta = 20$ and $\mathcal{O}_{12} = 0.05$. The shaded region satisfies all constraints in the Table.II, where triangle region on the right side of green curve is in the reach of HL-LHC (14 TeV, 3ab^{-1}) [18].

which implies that the EWSB is dominated by the Higgs doublet vevs of MSSM. In this situation, it is reasonable to ignore the $\sqrt{\delta}$ term in the scaling factor k_W and k_Z . Within the region with $10 \leq \tan\beta \leq 50$, a numerical scan imposed by the constraints in Table.II shows that

$$0.8 \leq \mathcal{O}_{11}^2 + \mathcal{O}_{12}^2 \leq 1.0 \tag{14}$$

for the values of δ in Eq.(13).

B. Higgs Self Coupling

Apart from the precision measurements on Higgs couplings as discussed above, a probe of Higgs self interaction is also useful in identifying the EWSB. In the SM, the tri-Higgs and quartic Higgs coupling reads as, respectively,

$$\begin{aligned}
\lambda_{3h}^{\text{SM}} &= \frac{3m_h^2}{v}, \\
\lambda_{4h}^{\text{SM}} &= \frac{3m_h^2}{v^2}.
\end{aligned} \tag{15}$$

The Higgs self coupling λ_{3h} is the key parameter to determine the SM Higgs pair production at LHC [22–26], since the cross section for Higgs pair production mainly arise from gluon gluon fusion. Comparing to SM, the cross section can be significantly altered in new physics such as MSSM and NMSSM even at tree level [22, 24, 27–30].

In our model, both λ_{3h} and λ_{4h} receive contributions from V_F and V_D . The contributions due to V_D are given

by,

$$\begin{aligned}\lambda_{3h_1} &= \frac{3M_Z^2}{v} \left[\sqrt{1-\delta}(\mathcal{O}_{11}^2 - \mathcal{O}_{12}^2)(s_\beta \mathcal{O}_{11} - c_\beta \mathcal{O}_{12}) \right. \\ &\quad \left. + \sqrt{\delta}(\mathcal{O}_{13}^2 - \mathcal{O}_{14}^2)(s_\gamma \mathcal{O}_{13} - c_\gamma \mathcal{O}_{14}) \right], \\ \lambda_{4h_1} &= \frac{3M_Z^2}{v^2} [(\mathcal{O}_{11}^2 - \mathcal{O}_{12}^2)^2 + (\mathcal{O}_{13}^2 - \mathcal{O}_{14}^2)^2].\end{aligned}\quad (16)$$

As shown in Eq.(14), the components \mathcal{O}_{11} and \mathcal{O}_{21} constitute most of SM-like Higgs within region with moderate or large $\tan\beta$ as required by Higgs mass. In comparison with \mathcal{O}_{11} and \mathcal{O}_{21} , components \mathcal{O}_{1j} ($j = 3 - 5$) can be ignored. Consider that the contributions to λ_{3h} and λ_{4h} due to V_F are at least of order \mathcal{O}_{1j}^2 , we will not include them in the following analysis. Note that the results in Eq.(16) reduce to those of MSSM in the decoupling limit $\delta \rightarrow 0$,

$$\begin{aligned}\lambda_{3h_1}^{\text{MSSM}} &= \frac{3M_Z^2}{v} \cos(2\alpha) \sin(\alpha + \beta), \\ \lambda_{4h_1}^{\text{MSSM}} &= \frac{3M_Z^2}{v^2} \cos^2(2\alpha).\end{aligned}\quad (17)$$

Thus, the probe of Higgs self interaction is useful in discriminating our model from either SM or MSSM.

With constraints on component \mathcal{O}_{11} and \mathcal{O}_{12} in the Table.II, we show in Fig.1 the contour of $\lambda_{3h}/\lambda_{3h}^{\text{SM}}$ for $\tan\beta = 20$ and $\mathcal{O}_{12} = 0.05$, with the shaded region satisfying all constraints in the Table.II. The ratio $\lambda_{3h}/\lambda_{3h}^{\text{SM}}$ is more sensitive to scaling factor δ and \mathcal{O}_{11} rather than \mathcal{O}_{12} for large $\tan\beta$. It reduces to the case of MSSM with $\delta \rightarrow 0$, in which case the maximal value $\lambda_{3h}^{\text{max}}/\lambda_{3h}^{\text{SM}} \sim 0.52$. In contrast, there is a suppression on the ratio when $\delta \neq 0$. The triangle region on the right side of green curve is in the reach of HL-LHC (14 TeV, 3ab⁻¹) [18], whereas the left side will be still invisible in the foreseeable future.

C. Higgs Mass

The soft mass parameters in Eq.(3) lead to mass splitting between fermion and its scalar partner in vectorlike superfield L , \bar{L} and N , which yield radioactive correction to Higgs mass. The correction to Higgs mass can be extracted via the one-loop correction to effective potential due to VL fields, which reads as [21],

$$\Delta V = 2 \sum_{i=1}^3 [F(M_{b_i}^2) - F(M_{f_i}^2)], \quad (18)$$

with $F(x) = x^2[\ln(x/Q^2) - 3/2]/64\pi^2$. For simplicity, we consider the universal soft masses $m_L = m_{\bar{L}} = m_N = m$, universal VL masses $M_L = M_{\bar{L}} = M_N = M$ and large $\tan\beta$ limit. Meanwhile, we take the good approximation $v_L = \bar{v}_L = 0$. The neutral scalar mass squared matrix, which determines the mass eigenvalues $M_{b_i}^2$ in Eq.(18), is

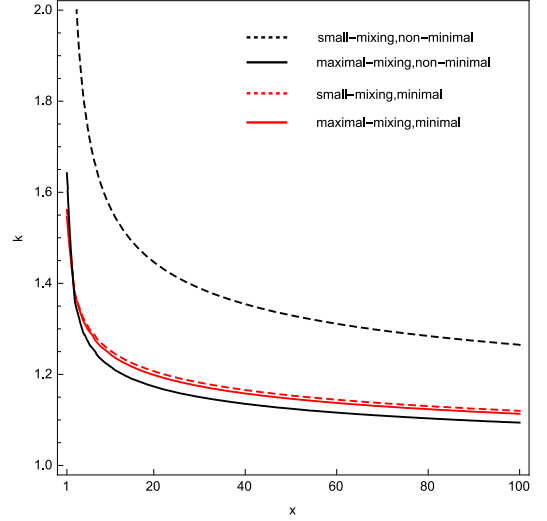


FIG. 2: The contour of Higgs mass with $\Delta M_h = \sqrt{(125 \text{ GeV})^2 - M_Z^2}$ as function of Yukawa coupling constant k and ratio $x = 1 + m^2/M^2$ that describes the mass splitting between scalars and fermions in the VL sector. The red and black curves refer to the minimal and non-minimal VL model, respectively.

given by (see Eq.(A1))

$$M_b^2 \simeq \begin{pmatrix} M^2 + m^2 & 0 & kMv_u \\ * & M^2 + m^2 + k^2v_u^2 & -kX_kv_u \\ * & * & M^2 + m^2 + k^2v_u^2 \end{pmatrix} \quad (19)$$

where $X_k \simeq M + A_k - \mu \cot\beta$. The neutral fermion mass squared matrix, which gives the mass eigenvalues $M_{f_i}^2$ in Eq.(18), reads as (see also Eq.(B3))

$$M_f^2 \simeq \begin{pmatrix} M^2 + k^2v_u^2 & 0 & kMv_u \\ * & M^2 & kMv_u \\ * & * & M^2 + k^2v_u^2 \end{pmatrix}, \quad (20)$$

Substituting mass eigenvalues in Eq.(19) and Eq.(20) into Eq.(18), we obtain the one-loop correction to SM-like Higgs mass

$$\begin{aligned}\Delta M_h^2 &\simeq \frac{1}{4\pi^2} k^4 v^2 \sin^4\beta \left[\ln(x) + \frac{1}{8} \left(\frac{\lambda(y)}{x} - \lambda_* \right) \right. \\ &\quad \left. - \frac{5}{192} \left(\frac{\lambda^2(y)}{x^2} - \lambda_*^2 \right) \right]\end{aligned}\quad (21)$$

where $x = 1 + m^2/M^2$, $y = X_k^2/M^2$ and $\lambda_* = \lambda(1)$, with $\lambda(y)$ defined as

$$\lambda(y) = 4 + 2y + 2\sqrt{y^2 + 4y}. \quad (22)$$

As clearly seen in Eq.(21), $\Delta M_h^2 \rightarrow 0$ under the degenerate mass limit $x \rightarrow 1$ and $y \rightarrow 1$, where the scalar and fermion masses are degenerate. Conversely, large ΔM_h^2 is expected in the situation with large x and certain value of

y. Fig.2 shows the contour of Higgs mass with correction $\Delta M_h = \sqrt{(125 \text{ GeV})^2 - M_Z^2}$. The red curves represent the minimal VL model, which are compared with the non-minimal VL model [9] as shown in black curves. In individual case, the dashed and solid one refers to the small- and large-mixing effect, respectively.

There are a few comments regarding the corrections to Higgs mass in these two VL models. First, X_k/M as fixed by the condition of maximal-mixing effect is equal to $12x/5$ and $2(3x-1)$ in the minimal and non-minimal VL model, respectively. Second, the discrepancies between the two VL models are small (large) in the situation with maximal (small)-mixing effect. Third, all of four patterns require large value of x , which implies that large mass splitting ($m/M \sim 10$) between scalars and fermions in the VL sector is favored if one wants the Yukawa coupling k staying in the perturbative region in high energy scales. For VL fermions of order $\sim 1 \text{ TeV}$, the VL scalars have mass of order $\sim 10 \text{ TeV}$, which have no role to play either at the LHC or dark matter experiments as what follows.

IV. DARK MATTER

In the MSSM with the minimal VL sector, the number of neutral fermions is seven, with four from the MSSM neutralino sector (for review, see, e.g.[31]) and the other three from the VL sector. The mass matrix for them is shown in Eq.(B3), where the complexity can be relatively reduced by taking the decoupling limit $v_L = \bar{v}_L = 0$ as favored by precise measurements on Higgs couplings. Moreover, a small but nonzero n is sufficient to yield desired decays in the VL sector, with the first-order approximation to which the mass matrix in Eq.(B3) is further divided into two separate parts -neutralino mass matrix A and VL mass matrix B .

A. VL Dark Matter

For VL dark matter $\tilde{\chi}_1^0$ is decomposed as,

$$\tilde{\chi}_1^0 = N_{15}^* \tilde{\eta} + N_{16}^* \tilde{\eta} + N_{17}^* \tilde{N}, \quad (23)$$

where for simplicity we have neglected the neutralinos in Eq.(B3). The mass matrix M_χ therein is reduced to matrix B . Since all of scalars in the VL sector are decoupled, the Lagrangian in Eq.(1) most relevant on our

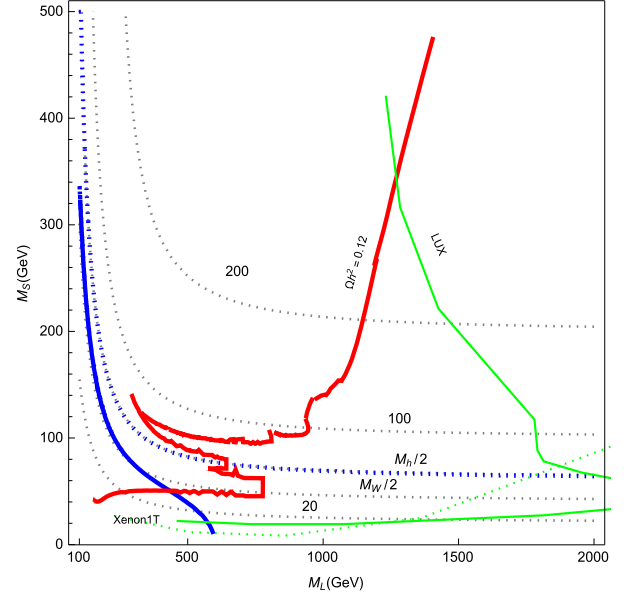


FIG. 3: Constraints on the parameter space of VL dark matter with $k = 1.2$ and $\tan \beta = 20$. The relic density of dark matter, the latest Xenon1T SI limit [40], LUX SD constraint [41], Z invisible decay limit [43], and Higgs invisible decay limit [44] is shown in red, green dotted, green solid, blue solid and blue dotted, respectively. The contours of VL dark matter masses in unit of GeV are shown in gray dotted curves.

discussion is given by¹,

$$\begin{aligned} \mathcal{L}_{\text{VL}} \supset & k(H_u^+ \tilde{E}^- - H_u^0 \tilde{\eta}) \tilde{N} - h(H_d^0 \tilde{\eta} - H_d^- \tilde{E}^+) \tilde{N} \\ & - \frac{g}{4c_W} \tilde{\eta} \gamma^\mu \gamma_5 \tilde{\eta} Z_\mu + \frac{g}{4c_W} \tilde{\eta} \gamma^\mu \gamma_5 \tilde{\eta} Z_\mu \\ & - \frac{g}{\sqrt{2}} \tilde{E}^+ \gamma^\mu P_L \tilde{\eta} W_\mu^+ + \frac{g}{\sqrt{2}} \tilde{E}^- \gamma^\mu P_R \tilde{\eta} W_\mu^-. \quad (24) \end{aligned}$$

Based on the simplifications above, the VL dark matter $\tilde{\chi}_1^0$ annihilation is mediated by Z boson, SM Higgs h_{SM} and the charged fermion \tilde{E}^\pm . Accordingly, the annihilation final states include SM fermions $\bar{f}f$, ZZ , WW and $h_{\text{SM}}h_{\text{SM}}$.

The Lagrangian in Eq.(24) shows that this VL dark matter model is a specific example of singlet-doublet dark matter [32–37]. In our case, the Yukawa coupling $k \simeq 1.1 - 1.2$ due to the observed Higgs mass, and h can be effectively neglected in the parameter region with $\tan \beta \geq 10$. Thus, there are only two free parameters M_L and M_N . As previously shown in e.g. ref.[37], the dark matter coupling to SM Higgs and Z boson is given

¹ We write both charged and neutral fermions in 4-component notation, e.g., $\chi_E^\pm = (\tilde{E}^\pm, \tilde{E}^\mp)$ and $\tilde{\chi}_1^0 = (\tilde{\chi}_1^0, \tilde{\chi}_1^0)$.

as respectively,

$$\begin{aligned} c_h &\simeq -\frac{k^2}{2} \frac{m_{\tilde{\chi}_1^0} v}{M_L^2 + \frac{k^2}{2} v^2 + 2M_N m_{\tilde{\chi}_1^0} - 3m_{\tilde{\chi}_1^0}^2}, \\ c_Z &\simeq -\frac{k^2}{2} \frac{M_Z v (m_{\tilde{\chi}_1^0}^2 - M_L^2)}{(m_{\tilde{\chi}_1^0}^2 - M_L^2)^2 + \frac{k^2}{2} v^2 (m_{\tilde{\chi}_1^0}^2 + M_L^2)}. \end{aligned} \quad (25)$$

Shown in Fig.3 is the constraints on the parameter space projected to the two-parameter plane of $M_L - M_S$ with $k = 1.2$. The red curve therein refers to the relic density of VL dark matter $\Omega h^2 \simeq 0.12$. Here, we handle the relic density of VL dark matter by the analytic method similar to ref.[37] instead of numerical treatments such as MicrOMEGAs [38]. We have used our previous analytic results in [39], where the cross sections for dark matter annihilations into various SM final states were derived. Meanwhile, we show the latest limits on the spin-independent (SI) and spin-dependent (SD) dark matter-p/n scattering cross sections from Xenon1T [40] and LUX [41], respectively. The SI and SD limits are projected to the plane of $M_L - M_S$ by using the results $\sigma_{SI} \simeq c_h^2 \times (2.11 \times 10^3)$ zb and $\sigma_{SD}^n \simeq c_z^2 \times (8.97 \times 10^8)$ zb. These limits are shown in green plots, above which the parameter regions are excluded. The VL dark matter is totally excluded by the latest Xenon1T limit. The main reason for this result is that large $k \sim 1.2$ and large $\tan \beta$ as both required by the 125 GeV Higgs mass lead to too large c_h in Eq.(25) to evade the Xenon1T limit.

In order to be concrete we also show in Fig.3 the indirect constraints² due to electroweak precision measurements [42] on Z and Higgs invisible decay widths $\Delta\Gamma_{h,Z}$. The experimental bounds $\Delta\Gamma_Z \leq 2$ MeV [43] and $\Delta\Gamma_h \leq 0.16\Gamma_h$ [44] are shown in blue solid and blue dotted curves, respectively. $\Delta\Gamma_h$ excludes the VL dark matter mass below $M_h/2$.

B. Neutralino Dark Matter

Although the VL dark matter is excluded, it still has a role to play in the case of neutralino dark matter. A neutralino dark matter $\tilde{\chi}_i^0$ mainly arises from following components:

$$\tilde{\chi}_i^0 = N_{i1}^* \tilde{B}^0 + N_{i2}^* \tilde{W}^0 + N_{i3}^* \tilde{H}_d^0 + N_{i4}^* \tilde{H}_u^0. \quad (26)$$

Its relic density is affected by the VL sector in the following ways.

Firstly, $\tilde{\chi}_1^0$ pair may annihilate into the VL final states such as $\tilde{E}^+ \tilde{E}^-$, through either the s -channel exchange of Z boson/Higgs scalar h_i or the t - and u -channel exchange

of VL scalars E^\pm . However, this channel is not kinetically allowed since the masses of \tilde{E}^\pm are larger than $m_{\tilde{\chi}_1^0}$ when \tilde{E}^\pm share the same R -parity³ as the neutralino $\tilde{\chi}_1^0$. Moreover, the t and u -channel exchange of VL scalars E^\pm are both suppressed by large VL scalar masses⁴ due to a large amount of radioactive correction to Higgs mass.

Also, the VL sector can mediate new Feynman diagrams for neutralino $\tilde{\chi}_1^0$ annihilation:

- Fermions \tilde{E}^\pm mediate t - or u - channel Feynman diagrams for neutralino annihilation into W^\pm , with the neutralino- χ_E^\pm - W vertex given by

$$\mathcal{L} \supset -\frac{g}{\sqrt{2}} W_\mu^- (N_{61} P_L - N_{51} P_R) \tilde{\chi}_1^0 \gamma^\mu \chi_E^+ + \text{H.c.} \quad (27)$$

- Fermions $\tilde{\eta}$ and $\tilde{\bar{\eta}}$ mediate t - or u - channel Feynman diagrams for neutralino annihilation into Z bosons, with the neutralino- $\tilde{\eta}/\tilde{\bar{\eta}}$ - Z vertex read as

$$\mathcal{L} \supset -\frac{g}{4c_W} Z_\mu \tilde{\chi}_1^0 \gamma^\mu \gamma_5 (N_{61} \tilde{\eta} - N_{51} \tilde{\bar{\eta}}) \quad (28)$$

- Fermions $\tilde{\eta}$, $\tilde{\bar{\eta}}$ and \tilde{N} mediate t - or u -channel Feynman diagrams for neutralino annihilation into hh , with the neutralino- $\tilde{\eta}/\tilde{\bar{\eta}}/\tilde{N}$ - h_{SM} vertex in the MSSM modified by

$$\begin{aligned} \mathcal{L} \supset & \frac{1}{\sqrt{2}} (-k N_{51} s_\beta + h N_{61} c_\beta) \tilde{\chi}_1^0 \tilde{N} h_{\text{SM}} \\ & + \frac{1}{\sqrt{2}} N_{71} (-k s_\beta \tilde{\eta} + h c_\beta \tilde{\eta}) \tilde{\chi}_1^0 h_{\text{SM}} \end{aligned} \quad (29)$$

Eq.(27) to Eq.(29) determine the deviation from ordinary neutralino, which rely on mixings between $\tilde{\chi}_1^0$ and VL sector as described by components N_{i1} with $i = 5 - 7$. With the mass parameter range $m \sim$ several TeVs, the conditions of EWSB in Eq.(9) imply that $\langle n \rangle$ is at most of order ~ 10 GeV and δ is less than ~ 0.01 . Thus, N_{i1} reaches to its maximal values in the case of higgsino-like $\tilde{\chi}_1^0$.

The effects on the higgsino-like $\tilde{\chi}_1^0$ can be divided into the VL doublets- and singlet-dominated correction. In the case of VL doublet-dominated correction, M_L is smaller than M_N . Modifications on the relic density of higgsino-like $\tilde{\chi}_1^0$ mainly arises from the neutralino- $\tilde{\eta}/\tilde{\bar{\eta}}$ - Z vertex, which also contributes to the SD cross section.

² Since the VL leptons do not directly mix with the SM leptons, in comparison with the electroweak precision measurements the other constraints such as lepton flavor violations are rather weak.

³ All the baryon and lepton numbers of L , \bar{L} and N are zero as inferred from Eq.(1). Thus, all of fermions in the VL sector are odd under the R -parity $(-1)^{3(B-L)+2s}$ similar to those of neutralinos and charginos. Mixing between the neutral (charged) fermions in the VL sector and neutralinos (charginos) in the MSSM always occur, unless different parity assignments are identified.

⁴ If there are other sources to uplift the Higgs mass, the VL scalar masses can be of order sub-TeV, in which situation this process deserves a detailed study [45, 46].

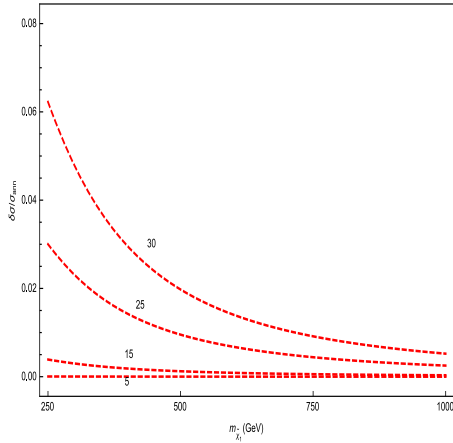


FIG. 4: In the case of VL doublet-dominated correction, the ratio $\delta\sigma_{\text{ann}}/\sigma_{\text{ann}}$ as function of higgsino-like neutralino mass $m_{\tilde{\chi}_1^0}$ for $-h = k = 1.2$, $|M_L - m_{\tilde{\chi}_1^0}| < M_Z$, and different values of $n = \{5, 15, 25, 30\}$ GeV, where $\sigma_{\text{ann}} \simeq 3 \times 10^{-27} \text{ cm}^3/\text{s}$.

The first-order solution to the reduced 4×4 mass matrix in Eq.(B3) only composed of Higgs doublets and VL doublets is given by

$$\begin{aligned} N_{61}^{\tilde{H}_{d(u)}} &\simeq -kn/(\mu + M_L), \\ N_{51}^{\tilde{H}_{d(u)}} &\simeq -(+)kn/(\mu + M_L), \\ N_{71}^{\tilde{H}_{d(u)}} &\simeq 0, \end{aligned} \quad (30)$$

for $h = -k$ and $M_N > M_L$. Substituting Eq.(30) into Eq.(28), we show the maximal correction to dark matter annihilation cross section σ_{ann} that occurs in the mass region $|M_L - m_{\tilde{\chi}_1^0}| < M_Z$ for different values of $n = \{5, 15, 25, 30\}$ GeV in Fig.4, where $k = 1.2$ is chosen as illustrated by Fig.2. It indicates that in the mass range of $m_{\tilde{\chi}_1^0} = 250 - 1000$ GeV, the ratio $\delta\sigma/\sigma_{\text{ann}}$ varies from 6% ($n = 30$ GeV) to less than 0.1% ($n = 5$ GeV). It is sensitive to n since $\delta\sigma$ is proportional to factor $(n/\mu + M_L)^4$. In the case of singlet-dominated correction, similar order of the ratio $\delta\sigma/\sigma_{\text{ann}}$ is also expected.

The modifications on neutralino relic density, SD and SI cross sections in percent level suggest that the parameter space of neutralino dark matter is mainly expanded in terms of relaxing the Higgs mass constraint e.g. by lowering the values of $\tan\beta$ or gaugino masses in the case of universal soft masses.

V. COLLIDER DETECTION

The VL lepton sector can be detected in different ways. If mixed with the SM leptons such as e , μ or τ , VL leptons can be constrained by mixing-relevant processes at collider constraints [47–49]. These constraints depend on both the VL lepton mass and its mixing with SM leptons. In our model, the VL leptons χ_E^\pm ($\tilde{\eta}$, $\tilde{\bar{\eta}}$) directly mix

Signals	Background
$\chi_E^+ \chi_E^-$ [50]	(jets)+ leptons + E_T^{miss}
$\tilde{\eta}$ or $\tilde{\bar{\eta}}$ pair [51]	jets+ (leptons) + E_T^{miss}
$\chi_E^\pm + \tilde{\eta}$ or $\chi_E^\pm + \tilde{\bar{\eta}}$ [52, 53]	(jets)+ leptons + E_T^{miss}

TABLE III: SM backgrounds for VL lepton pairs, where E_T^{miss} refers to missing transverse momentum.

with charginos (neutralinos) rather than SM leptons, the strategy of searching them at colliders thus differs from the case of lepton mixings.

The VL leptons can be produced via chargino (neutralino) decay when their masses are beneath chargino (neutralino) masses. or they just imitate the electroweak productions of charginos (neutralinos). The main difference between these two processes are that the cross section for the former case depends on both the VL lepton masses and their mixings with chargino or neutralinos, while the cross section for the later one mainly relies on the VL lepton pair masses. Here, we stick to the later case, in which the main final states contain lepton pairs composed of χ_E^\pm , $\tilde{\eta} + \tilde{\bar{\eta}}$, $\chi_E^\pm + \tilde{\eta}$ and $\chi_E^\pm + \tilde{\bar{\eta}}$.

We show the SM backgrounds for different lepton pairs at LHC in Tabel.III. All of these lepton pairs can decay into SM leptons with missing energy in terms of Z -, W - or Higgs-mediated decays $\chi_E^\pm \rightarrow \tilde{\chi}_1^0$ and $\tilde{\chi}_2^0 \rightarrow \tilde{\chi}_1^0$. So, there are a number of processes in which both the productions and decays of lepton pairs occur through Z or W boson. These processes are only sensitive to the mass parameters related to lepton pairs, because the vertexes of interactions are mostly fixed by gauge interactions. We will discuss the prospect on this class of signals at HL-LHC elsewhere in detail.

VI. CONCLUSION

In this paper, we have studied the minimal VL model from conventional grand unification. The key feature in such model is that the VL leptons only couple to the Higgs doublets rather than mix with SM leptons. Therefore, they have important roles to play in the phenomenologies of both Higgs physics and dark matter.

For the Higgs physics, we have used the LHC bounds on the Higgs coupling constants to constrain the vevs restored in the VL sector, the magnitude of which are found to be small. Consequently, the magnitudes of the mixing effects between the Higgs doublets and the VL sector controlled by the vevs are small as well, leading to small deviation in the Higgs self coupling from the MSSM expectation. We also used the observed Higgs mass to constrain the other model parameters in the VL sector. The fit reveals that both large Yukawa coupling constant $k \sim 1.1 - 1.2$ and large mass splitting of order one in the VL sector are required to uplift the Higgs mass.

Having obtained the first-hand information about the

model parameters, we continued to address the dark matter phenomenology. We found the large Yukawa coupling k excludes the possibility of VL dark matter. For it gives rise to too large dark matter coupling to the Higgs to evade the Xenon1T limit. Nevertheless, they are still useful to reduce the stress on the neutralino dark matter by relaxing the constraint on Higgs mass.

In order to be complete, we briefly discuss the constraints on such VL leptons at the LHC. Unlike the SM lepton mixing-relevant processes, VL leptons can be produced via the decays of charginos and neutralinos, or just imitate the electroweak productions of them. The prospect on the second class of productions at the HL-LHC deserves more detailed studies.

Acknowledgments. We would like to thank Prof. P. Fayet for correspondence and Dr. H. Wu for a numerical check on the case of neutralino dark matter. The research is supported by the National Natural Science Foundation of China with Grant No.11775039 and the Fundamental Research Funds for the Central Universities at Chongqing University with Grant No.cqu2017hbrclB05.

Appendix A: Scalar Mass Matrix

1. CP-even Scalar

In the basis $\phi_S^T = (H_{uR}^0, H_{dR}^0, \eta_R, \bar{\eta}_R, N_R)$, the matrix elements for symmetric mass matrix squared \mathcal{M}_S^2 of CP-even scalars in the Lagrangian

$$\mathcal{L} \supset \frac{1}{2} \phi_S^{T,i} \mathcal{M}_{S,ij}^2 \phi_S^j \quad (\text{A1})$$

are as follows,

$$\begin{aligned} \mathcal{M}_{S,11}^2 &= \mu^2 + m_{H_u}^2 + k^2(n^2 + \bar{v}_L^2) \\ \mathcal{M}_{S,12}^2 &= b - khv_L \bar{v}_L \\ \mathcal{M}_{S,13}^2 &= -hn\mu - kh\bar{v}_L v_d + kM_L n \\ \mathcal{M}_{S,14}^2 &= 2k^2 v_u \bar{v}_L + k(M_N n + hv_d v_L) - kA_k n \\ \mathcal{M}_{S,15}^2 &= 2k^2 n v_u - hv_L \mu - kM_N \bar{v}_L + kM_L v_L - kA_k \bar{v}_L \\ \mathcal{M}_{S,22}^2 &= \mu^2 + m_{H_d}^2 + h^2(n^2 + v_L^2) \\ \mathcal{M}_{S,23}^2 &= 2h^2 v_d v_L + h(M_N n - kv_u \bar{v}_L) - hA_h n \\ \mathcal{M}_{S,24}^2 &= kn\mu - khv_u v_L - hM_L n \\ \mathcal{M}_{S,25}^2 &= 2h^2 n v_d + k\bar{v}_L \mu + hM_N v_L + hM_L \bar{v}_L + hA_k v_L \\ \mathcal{M}_{S,33}^2 &= M_L^2 + m_L^2 + h^2(n^2 + v_d^2) \\ \mathcal{M}_{S,34}^2 &= -khv_u v_d \\ \mathcal{M}_{S,35}^2 &= 2h^2 n v_L - hv_u \mu + hM_N v_d + kM_L v_u + hA_h v_d \\ \mathcal{M}_{S,44}^2 &= M_L^2 + m_L^2 + k^2(n^2 + v_u^2) \\ \mathcal{M}_{S,45}^2 &= 2k^2 n \bar{v}_L + kv_d \mu - kM_N v_u - hM_L v_d - kA_k v_u \\ \mathcal{M}_{S,55}^2 &= M_N^2 + m_N^2 + h^2(v_L^2 + v_d^2) + k^2(\bar{v}_L^2 + v_u^2) \quad (\text{A2}) \end{aligned}$$

where D -term contributions have been neglected. After diagonalizing the matrix \mathcal{M}_S^2 , we obtain five physical neutral scalars, one of which serves as the SM-like Higgs boson h with mass 125 GeV [1, 2].

2. CP-odd Scalar

In the basis $\phi_A^T = (H_{uI}, H_{dI}, \eta_I, \bar{\eta}_I, N_I)$ the matrix elements for CP-odd scalars in the Lagrangian

$$\mathcal{L} \supset \frac{1}{2} \phi_A^{T,i} \mathcal{M}_{A,ij}^2 \phi_A^j \quad (\text{A3})$$

are given by,

$$\begin{aligned} \mathcal{M}_{A,11}^2 &= \mu^2 + m_{H_u}^2 + k^2(n^2 + \bar{v}_L^2) \\ \mathcal{M}_{A,12}^2 &= b - khv_L \bar{v}_L \\ \mathcal{M}_{A,13}^2 &= -hn\mu - kh\bar{v}_L v_d + kM_L n \\ \mathcal{M}_{A,14}^2 &= -k(M_N n + hv_d v_L) + kA_k n \\ \mathcal{M}_{A,15}^2 &= -hv_L \mu - kM_N \bar{v}_L - kM_L v_L + kA_k \bar{v}_L \\ \mathcal{M}_{A,22}^2 &= \mu^2 + m_{H_d}^2 + h^2(n^2 + v_L^2) \\ \mathcal{M}_{A,23}^2 &= -h(M_N n - kv_u \bar{v}_L) - hA_h n \\ \mathcal{M}_{A,24}^2 &= kn\mu - khv_u v_L - hM_L n \\ \mathcal{M}_{A,25}^2 &= +k\bar{v}_L \mu + hM_N v_L - hM_L \bar{v}_L - hA_k v_L \\ \mathcal{M}_{A,33}^2 &= M_L^2 + m_L^2 + h^2(n^2 + v_d^2) \\ \mathcal{M}_{A,34}^2 &= -khv_u v_d \\ \mathcal{M}_{A,35}^2 &= hv_u \mu + hM_N v_d + kM_L v_u - hA_h v_d \\ \mathcal{M}_{A,44}^2 &= M_L^2 + m_L^2 + k^2(n^2 + v_u^2) \\ \mathcal{M}_{A,45}^2 &= -kv_d \mu - kM_N v_u - hM_L v_d + kA_k v_u \\ \mathcal{M}_{A,55}^2 &= M_N^2 + m_N^2 + h^2(v_L^2 + v_d^2) + k^2(\bar{v}_L^2 + v_u^2) \quad (\text{A4}) \end{aligned}$$

where the D -term contributions have been neglected. Under the decoupling limit $v_L = \bar{v}_L = 0$ and $n = 0$, scalar η_I , $\bar{\eta}_I$ and N_I decouple from H_{uI} and H_{dI} , which results in the well known result $\text{Det} \mathcal{M}_A^2 = 0$.

3. CP-charged Scalar

In the basis $\phi_c^T = (H_u^+, H_d^{*-}, E^+, E^{-*})$ the matrix elements for charged scalars in the Lagrangian

$$\mathcal{L} \supset \phi_c^{*T,i} \mathcal{M}_{C,ij}^2 \phi_c^j \quad (\text{A5})$$

read as

$$\begin{aligned}
\mathcal{M}_{C,11}^2 &= \mu^2 + m_{H_u}^2 + k^2(n^2 + \bar{v}_L^2) \\
\mathcal{M}_{C,12}^2 &= -khv_L\bar{v}_L \\
\mathcal{M}_{C,13}^2 &= -hn\mu - kh\bar{v}_Lv_d + kM_Ln \\
\mathcal{M}_{C,14}^2 &= k(M_Nn - hv_dv_L) + kA_kn \\
\mathcal{M}_{C,22}^2 &= \mu^2 + m_{H_d}^2 + h^2(n^2 + v_L^2) \\
\mathcal{M}_{C,23}^2 &= -h(M_Nn - kv_u\bar{v}_L) - hA_hn \\
\mathcal{M}_{C,24}^2 &= kn\mu - khv_uv_L - hM_Ln \\
\mathcal{M}_{C,33}^2 &= M_L^2 + m_L^2 + h^2(n^2 + v_d^2) \\
\mathcal{M}_{C,34}^2 &= -khv_uv_d \\
\mathcal{M}_{C,44}^2 &= M_L^2 + m_L^2 + k^2(n^2 + v_u^2) \quad (\text{A6})
\end{aligned}$$

Under the decoupling limit $v_L = \bar{v}_L = 0$ and $n = 0$, scalar E^+ and E^{*-} decouple from the others, due to which one recovers the relation $\text{Det}\mathcal{M}_C^2 = 0$.

Appendix B: Fermion Mass Matrix

1. Charged Fermions

In the basis $\chi_\pm^T = (\tilde{W}^+, \tilde{H}_u^+, \tilde{E}^+, \tilde{W}^-, \tilde{H}_d^-, \tilde{E}^-)$ the mass matrix in $\mathcal{L} \supset -\frac{1}{2}\chi_\pm^{T,i}\mathcal{M}_{\chi^\pm,ij}\chi_\pm^j$ is given by,

$$\mathcal{M}_{\chi^\pm,ij} = \begin{pmatrix} 0 & X^T \\ X & 0 \end{pmatrix} \quad (\text{B1})$$

with

$$X = \begin{pmatrix} M_2 & \sqrt{2(1-\delta)}s_\beta M_W & \sqrt{2\delta}s_\gamma M_W \\ \sqrt{2(1-\delta)}c_\beta M_W & \mu & -hn \\ \sqrt{2\delta}c_\gamma M_W & kn & M_L \end{pmatrix} \quad (\text{B2})$$

where $s_\beta = \sin \beta$, $c_\beta = \cos \beta$, $s_\gamma = \sin \gamma$ and $c_\gamma = \cos \gamma$.

2. Neutral Fermions

In the basis $\psi_0^T = (\tilde{B}^0, \tilde{W}^0, \tilde{H}_d^0, \tilde{H}_u^0, \tilde{\eta}, \tilde{\eta}, \tilde{N})$ the mass matrix in $\mathcal{L} \supset -\frac{1}{2}\psi_0^{T,i}\mathcal{M}_{\chi,ij}\psi_0^j$ reads as,

$$M_\chi = \begin{pmatrix} A & C \\ * & B \end{pmatrix}, \quad (\text{B3})$$

with

$$\begin{aligned}
A &= \begin{pmatrix} M_1 & 0 & -(1-\delta)M_Z s_W c_\beta & (1-\delta)M_Z s_W s_\beta \\ * & M_2 & (1-\delta)M_Z c_W c_\beta & -(1-\delta)M_Z c_W s_\beta \\ * & * & 0 & -\mu \\ * & * & * & 0 \end{pmatrix}, \\
B &= \begin{pmatrix} 0 & -M_L & -kv_u \\ * & 0 & hv_d \\ * & * & -M_N \end{pmatrix}, \\
C &= \begin{pmatrix} -\delta M_Z s_W c_\gamma & \delta M_Z s_W s_\gamma & 0 \\ \delta M_Z c_W c_\gamma & -\delta M_Z c_W s_\gamma & 0 \\ 0 & hn & hv_L \\ -kn & 0 & -k\bar{v}_L \end{pmatrix}. \quad (\text{B4})
\end{aligned}$$

-
- [1] G. Aad *et al.* [ATLAS Collaboration], Phys. Lett. **B716**, 1 (2012), [arXiv:1207.7214 [hep-ex]].
 - [2] S. Chatrchyan *et al.* [CMS Collaboration], Phys. Lett. **B716**, 30 (2012), [arXiv:1207.7235 [hep-ex]].
 - [3] M. Carena, S. Gori, N. R. Shah and C. E. M. Wagner, JHEP **1203**, 014 (2012), [arXiv:1112.3336 [hep-ph]].
 - [4] L. J. Hall, D. Pinner and J. T. Ruderman, JHEP **1204**, 131 (2012), [arXiv:1112.2703 [hep-ph]].
 - [5] H. Baer, V. Barger and H. Serce, Phys. Rev. D **94**, no. 11, 115019 (2016), [arXiv:1609.06735 [hep-ph]].
 - [6] J. Cao, Y. He, L. Shang, W. Su, P. Wu and Y. Zhang, JHEP **1610**, 136 (2016), [arXiv:1609.00204 [hep-ph]].
 - [7] S. Zheng, Phys. Rev. D **98**, 035028 (2018), [arXiv:1711.05362 [hep-ph]].
 - [8] S. Zheng, Eur. Phys. J. C **77**, no. 9, 588 (2017), [arXiv:1706.01071 [hep-ph]].
 - [9] S. P. Martin, Phys. Rev. D **81**, 035004 (2010), [arXiv:0910.2732 [hep-ph]].
 - [10] T. Moroi and Y. Okada, Phys. Lett. B **295**, 73 (1992).
 - [11] K. S. Babu, I. Gogoladze, M. U. Rehman and Q. Shafi, Phys. Rev. D **78**, 055017 (2008).
 - [12] P. Fayet, Nucl. Phys. B **90**, 104 (1975).
 - [13] S. P. Martin, Adv. Ser. Direct. High Energy Phys. **21**, 1 (2010), [hep-ph/9709356].
 - [14] A. M. Sirunyan *et al.* [CMS Collaboration], Phys. Lett. B **780**, 501 (2018), [arXiv:1709.07497 [hep-ex]].
 - [15] G. Aad *et al.* [ATLAS Collaboration], JHEP **1504**, 117 (2015), [arXiv:1501.04943 [hep-ex]].
 - [16] G. Aad *et al.* [ATLAS Collaboration], Phys. Rev. D **92**, no. 1, 012006 (2015), [arXiv:1412.2641 [hep-ex]].
 - [17] J. Ellis and T. You, JHEP **1306**, 103 (2013), [arXiv:1303.3879 [hep-ph]].

- [18] S. Dawson *et al.*, [arXiv:1310.8361 [hep-ex]].
- [19] D. M. Asner *et al.*, [arXiv:1310.0763 [hep-ph]].
- [20] V. Khachatryan *et al.* [CMS Collaboration], *Eur. Phys. J. C* **75**, no. 5, 212 (2015), [arXiv:1412.8662 [hep-ex]].
- [21] S. R. Coleman and E. J. Weinberg, *Phys. Rev. D* **7**, 1888 (1973).
- [22] T. Plehn, M. Spira and P. M. Zerwas, *Nucl. Phys. B* **479**, 46 (1996), Erratum: [*Nucl. Phys. B* **531**, 655 (1998)], [hep-ph/9603205].
- [23] E. W. N. Glover and J. J. van der Bij, *Nucl. Phys. B* **309**, 282 (1988).
- [24] S. Dawson, S. Dittmaier and M. Spira, *Phys. Rev. D* **58**, 115012 (1998), [hep-ph/9805244].
- [25] J. Grigo, J. Hoff, K. Melnikov and M. Steinhauser, *Nucl. Phys. B* **875**, 1 (2013), [arXiv:1305.7340 [hep-ph]].
- [26] D. de Florian and J. Mazzitelli, *Phys. Rev. Lett.* **111**, 201801 (2013), [arXiv:1309.6594 [hep-ph]].
- [27] N. D. Christensen, T. Han and T. Li, *Phys. Rev. D* **86**, 074003 (2012), [arXiv:1206.5816 [hep-ph]].
- [28] R. Barbieri, D. Buttazzo, K. Kannike, F. Sala and A. Tesi, *Phys. Rev. D* **87**, no. 11, 115018 (2013), [arXiv:1304.3670 [hep-ph]].
- [29] R. S. Gupta, H. Rzehak and J. D. Wells, *Phys. Rev. D* **88**, 055024 (2013), [arXiv:1305.6397 [hep-ph]].
- [30] L. Wu, J. M. Yang, C. P. Yuan and M. Zhang, *Phys. Lett. B* **747**, 378 (2015), [arXiv:1504.06932 [hep-ph]].
- [31] G. Jungman, M. Kamionkowski and K. Griest, *Phys. Rept.* **267**, 195 (1996), [hep-ph/9506380].
- [32] R. Mahbubani and L. Senatore, *Phys. Rev. D* **73**, 043510 (2006), [hep-ph/0510064].
- [33] F. D'Eramo, *Phys. Rev. D* **76**, 083522 (2007), [arXiv:0705.4493 [hep-ph]].
- [34] R. Enberg, P. J. Fox, L. J. Hall, A. Y. Papaioannou and M. Papucci, *JHEP* **0711**, 014 (2007), [arXiv:0706.0918 [hep-ph]].
- [35] T. Cohen, J. Kearney, A. Pierce and D. Tucker-Smith, *Phys. Rev. D* **85**, 075003 (2012), [arXiv:1109.2604 [hep-ph]].
- [36] C. Cheung and D. Sanford, *JCAP* **1402**, 011 (2014), [arXiv:1311.5896 [hep-ph]].
- [37] L. Calibbi, A. Mariotti and P. Tziveloglou, *JHEP* **1510**, 116 (2015), [arXiv:1505.03867 [hep-ph]].
- [38] G. Belanger, F. Boudjema, A. Pukhov and A. Semenov, *Comput. Phys. Commun.* **192**, 322 (2015), arXiv:1407.6129 [hep-ph].
- [39] H. Han, H. Wu and S. Zheng, *Chin. Phys. C* **43**, 043103 (2019), [arXiv:1711.10097 [hep-ph]].
- [40] E. Aprile *et al.* [XENON Collaboration], *Phys. Rev. Lett.* **121**, no. 11, 111302 (2018), [arXiv:1805.12562 [astro-ph.CO]].
- [41] D. S. Akerib *et al.* [LUX Collaboration], *Phys. Rev. Lett.* **118**, no. 25, 251302 (2017), [arXiv:1705.03380 [astro-ph.CO]].
- [42] F. del Aguila, J. de Blas and M. Perez-Victoria, *Phys. Rev. D* **78**, 013010 (2008), [arXiv:0803.4008 [hep-ph]].
- [43] S. Schael *et al.* [ALEPH and DELPHI and L3 and OPAL and SLD Collaborations and LEP Electroweak Working Group and SLD Electroweak Group and SLD Heavy Flavour Group], *Phys. Rept.* **427**, 257 (2006), [hep-ex/0509008].
- [44] G. Aad *et al.* [ATLAS and CMS Collaborations], *JHEP* **1608**, 045 (2016), [arXiv:1606.02266 [hep-ex]].
- [45] M. Abdullah, J. L. Feng, S. Iwamoto and B. Lillard, *Phys. Rev. D* **94**, no. 9, 095018 (2016), [arXiv:1608.00283 [hep-ph]].
- [46] J. Y. Araz, S. Banerjee, M. Frank, B. Fuks, A. Goudelis, arXiv:1810.07224 [hep-ph].
- [47] G. Aad *et al.* [ATLAS Collaboration], *JHEP* **1509**, 108 (2015), [arXiv:1506.01291 [hep-ex]].
- [48] P. Achard *et al.* [L3 Collaboration], *Phys. Lett. B* **517**, 75 (2001), [hep-ex/0107015].
- [49] N. Kumar and S. P. Martin, *Phys. Rev. D* **92**, no. 11, 115018 (2015), [arXiv:1510.03456 [hep-ph]].
- [50] G. Aad *et al.* [ATLAS Collaboration], *JHEP* **1405**, 071 (2014), [arXiv:1403.5294 [hep-ex]].
- [51] V. Khachatryan *et al.* [CMS Collaboration], *Phys. Rev. D* **90**, no. 9, 092007 (2014), [arXiv:1409.3168 [hep-ex]].
- [52] G. Aad *et al.* [ATLAS Collaboration], *Eur. Phys. J. C* **75**, no. 5, 208 (2015), [arXiv:1501.07110 [hep-ex]].
- [53] M. Aaboud *et al.* [ATLAS Collaboration], *Eur. Phys. J. C* **78**, no. 12, 995 (2018), [arXiv:1803.02762 [hep-ex]].